

Entrance Channel Phenomena in Complex Nuclear Scattering*

A. Gobbi,† R. Wieland, L. Chua, D. Shapira, and D. A. Bromley

A. W. Wright Nuclear Structure Laboratory, Yale University, New Haven, Connecticut 06520

(Received 22 August 1972)

The elastic scattering excitation functions of the systems ${}^6\text{Li}-{}^6\text{Li}$, ${}^{12}\text{C}-{}^{12}\text{C}$, ${}^{14}\text{N}-{}^{14}\text{N}$, ${}^{16}\text{O}-{}^{14}\text{N}$, ${}^{16}\text{O}-{}^{15}\text{N}$, ${}^{16}\text{O}-{}^{16}\text{O}$, ${}^{16}\text{O}-{}^{18}\text{O}$, and ${}^{18}\text{O}-{}^{18}\text{O}$ have been subjected to comparative optical-model analyses. The gross structure characteristic of all these excitation functions is shown to arise from potential scattering phenomena. These phenomena have been studied in detail. The extracted ${}^{16}\text{O}-{}^{16}\text{O}$ potential has been used as input to detailed studies leading to the identification of single partial-wave orbiting resonances of 3- to 4-MeV width. The ${}^{16}\text{O}-{}^{16}\text{O}$ experimental data have also been used to test for the possible existence of a variable-moment-of-inertia effect during the interpenetrating collisions; no evidence for such an effect has been found, at least in this particular case. New suggestions for the prediction of the imaginary optical-potential parameters have been investigated.

I. INTRODUCTION

In recent years with increasing availability of heavy-ion accelerator facilities, an extensive body of experimental data concerning the elastic scattering of complex nuclear systems – heavy-ion scattering – has been accumulated. Thus far, however, the amount of specifically nuclear information which has been extracted from these data has been severely limited by inadequate understanding of the entrance channel characteristics in these scattering interactions. Inasmuch as these entrance channel phenomena play a central role in all nuclear interactions involving complex nuclei, it becomes of great importance to understand and parametrize the phenomena involved so that they may be unfolded from the experimental information on more complex interactions to yield the desired nuclear information.

In this paper we report on one phase of a systematic study of heavy-ion elastic scattering which we have undertaken in this laboratory. With our own measurements and those now available from other laboratories there exists a sufficient body of information to make possible at least an initial examination of the dependence of the entrance channel phenomena upon such parameters as nuclear mass, nuclear deformation, nuclear collectivity, and the like.

As has been repeatedly emphasized in scattering studies in the past, the direct determination of a complex interaction potential from the scattering phases extracted from measured cross sections is plagued with ambiguities, both discrete and continuous, in the parameters involved. In an effort to understand certain of these ambiguities more clearly, we consider herein the uniquely determined inverse problem where, given a poten-

tial which provides a reasonable reproduction of experimental data, we analyze in detail its precise cross-section predictions.

Of particular interest has been the demonstration of the importance of orbiting resonances in the heavy-ion interactions at energies in the vicinity of the potential barriers. These orbiting resonances were predicted many years ago¹; however, we believe that our present heavy-ion observations constitute the most clear cut example which has yet been reported. Although the orbiting resonances involve single partial waves and thus require a full quantum-mechanical description, their general features are very closely related to well-known classical and quasiclassical orbiting phenomena. We have examined the conditions necessary for this orbiting in some detail in terms of an extension of the l -dependent absorptive interaction initially suggested by Robson and his collaborators.²

To gain further insight into the connection between the potential model parameters and the predicted cross sections we have carried through a direct phase-shift parametrization of the ${}^{16}\text{O} + {}^{16}\text{O}$ scattering interaction, very similar to that proposed a number of years ago by McIntyre and his collaborators.³ This has permitted us to search for the possible existence of a variable moment of inertia for the strongly interacting system; as yet no evidence in support of such an effect has been found.

We report on a preliminary attempt at parametrizing the absorptive part of the optical model in terms of appropriately averaged parameters, as, for example, the compound system level density, for the nuclear systems involved. Promising results have been obtained.

We conclude the paper with an examination of

the present limitations of the models available for the description of heavy-ion elastic scattering and indicate some of the outstanding problems and uncertainties which remain before a complete understanding of the entrance channel in these important interactions can be achieved.

II. EXPERIMENTAL RESULTS ON ELASTIC SCATTERING OF COMPLEX NUCLEI

Although considerable early information was obtained on the angular distribution at fixed energy for a large number of heavy-ion scattering situations,⁴ we shall focus herein on measurements wherein the energy dependence of the elastic scattering cross sections are available. As we have indicated in earlier reports,⁵ and as has been found elsewhere, the experimental excitation functions have shown a wide range of interesting and often unexpected phenomena. It has been found⁶ that by focusing on simultaneously measured excitation functions, at a number of angles of observation and requiring systematic reproduction of the energy dependence of the cross sections of all these angles of observation, it becomes possible to substantially eliminate the confusion and often totally erroneous conclusions which result from theoretical study of isolated angular distributions. This confusion, of course, reflects the fact that phenomena measured at a single sharply defined energy can be grossly conditioned by fluctuation phenomena and may be totally nonrepresentative of the averaged interaction parameters.

We have also found that an angle-energy map of the differential cross section makes possible the elimination of a large fraction of the well-known ambiguities in the scattering potentials which were noted above. Beyond that, the map has been found to be extremely helpful in addressing a variety of more specific questions concerning the angular momentum and energy dependence of the potential parameters, the possible existence of a hard core in the nuclear potential, the possible variation of the moment of inertia of the interacting system, and the identification of possible quasimolecular or exchange phenomena in the scattering.

In the work in this laboratory we have focused primarily on the scattering of identical particles in order to simplify the situation as much as possible; the removal of all odd partial waves from the interaction, which characterizes such situations, greatly facilitates the analysis and the identification of specific phenomena in the scattering which in many cases are completely masked if all partial waves participate simultaneously.

In order to be able to compare the experimental

data for both identical and nonidentical systems on a common basis, we shall begin the present discussion by considering only the 90° excitation functions. It can readily be shown that at $\theta=90^\circ$ Mott scattering, characteristic of identical particles, reduces to familiar Rutherford scattering.

Figure 1 shows that all of the presently available data on excitation functions⁶⁻¹³ present a sim-

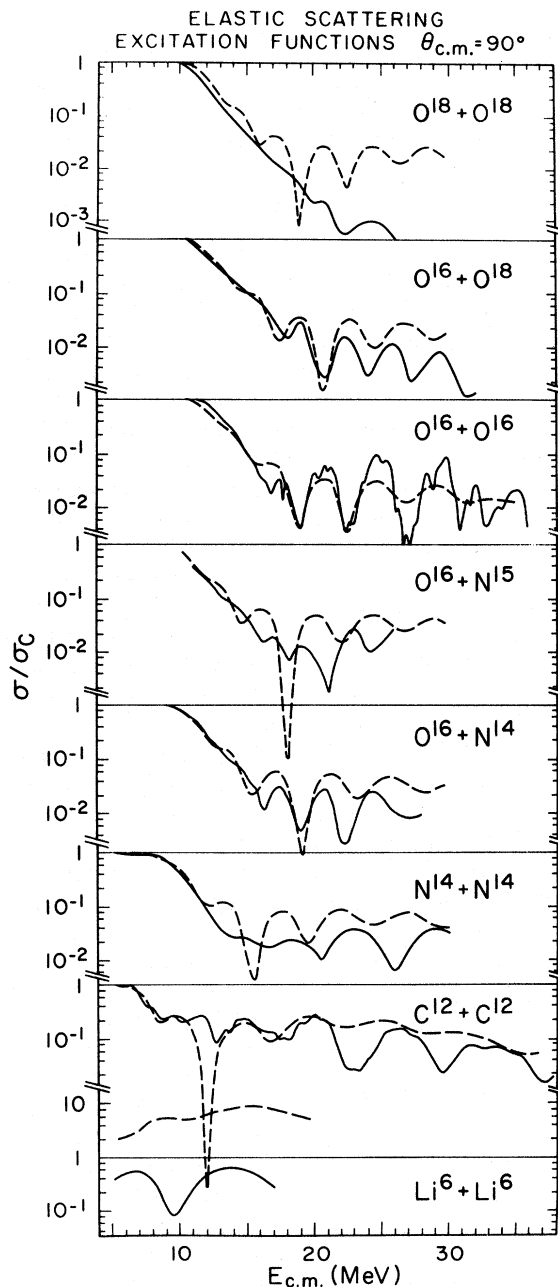


FIG. 1. Collected heavy-ion elastic scattering excitation functions. The full lines represent data while the dashed lines are optical-model predictions.

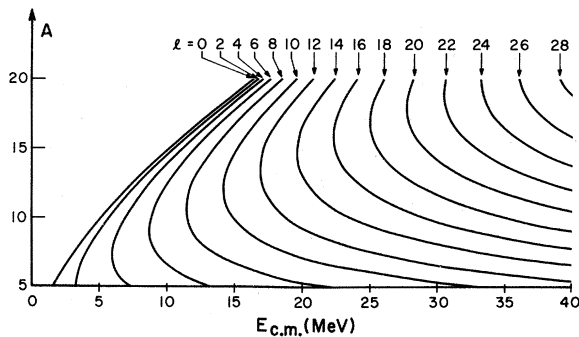


FIG. 2. Schematic plot of the angular momenta in a surface collision of identical nuclei as function of the mass and energy involved. Pure Coulomb scattering is assumed with $Z = \frac{1}{2}A$.

ilar gross structure which is typically a few MeV in width. It should be noted that the presently available heavy-ion accelerating facilities have restricted the data to the p shell and the low end of the sd shell. It will be extremely important, as higher-energy tandem Van de Graaff accelerators become available and as more ready energy variability becomes possible with the larger cyclotrons, to extend such measurements to much heavier nuclei where new and important phenomena can be expected to emerge.

In this paper we shall focus on an understanding of the gross structure in such excitation functions and its source. Both the structure of intermediate width (~ 200 keV) and possible fine fluctuation phenomena which is not apparent on the scale to which Fig. 1 is drawn, reflect more complex mechanisms and will be considered in later publications. Inasmuch as the focus here is on the gross structure, the $^{12}\text{C} + ^{12}\text{C}$ data, for example, have been energy averaged to emphasize these aspects.

It should first be noted that the characteristic width of the gross structure decreases systematically in going to heavier systems. We shall return to this point below. Only the nonidentical $^{16}\text{O} + ^{14}\text{N}$ and $^{16}\text{O} + ^{15}\text{N}$ systems appear as exceptions.

A wide variety of optical-model calculations have been undertaken to interpret and reproduce^{6, 8, 14-18} the gross structure, particularly that initially reported in the $^{16}\text{O} + ^{16}\text{O}$ system. The dashed curves of Fig. 1 are the optical-model predictions based on the Woods-Saxon optical-model parameters reported by Maher *et al.*⁶ in their original work on the $^{16}\text{O} + ^{16}\text{O}$ scattering. In applying these optical-model parameters to the different systems shown in Fig. 1, only the interaction radius was changed (scaled as $A^{1/3}$). Although even this simple model does produce a correct width for the gross structure, the exact positions of maxima and minima,

as well as their relative magnitudes, cannot be reproduced without more precise matching of the parameters to the individual nuclear channel studied. Reflecting the fact that the original Maher parameters were determined for the strongly bound $^{16}\text{O} + ^{16}\text{O}$ system, the predicted cross sections extrapolated to all other systems shown in Fig. 1 lie above the measured values.

The systematic change in the periodicity of the gross structure as a function of the mass of the ions in the entrance channel may be understood qualitatively by examining the maximum angular momentum expected in the interaction as a function of both the bombarding energy and the masses involved. Figure 2 presents such a representation for the idealized case of a surface collision of identical particles in a pure Coulomb field; the distance of closest approach has been taken as appropriate to a radius constant $r_0 = 1.6$ fm. The indicated barriers include both centrifugal and Coulomb effects. For smaller-mass ions the centrifugal effects dominate because of the reduced interaction radius; with increasing mass the Coulomb effects become more important and the figure indicates the transition as a function of increasing bombarding energy between Fresnel diffraction where the Coulomb distortion effects are dominant and Fraunhofer diffraction where the bombarding energy can be considered large as compared to the Coulomb energies of the problem. The direct and interesting analogy between heavy-ion scattering and physical optics has been examined most recently by Frahn.¹⁹

As is clear from Fig. 2 it can be argued that the gross structure observed in the experimental excitation functions reflects the systematic introduction of new partial waves into the scattering problem as the scattering energy is increased. Although this is an extremely crude viewpoint, it receives support from much more detailed considerations which we shall present below.

III. OPTICAL-MODEL ANALYSES: IDENTICAL PARTICLE SYSTEMS

We return in Fig. 3 to the original series of five excitation functions for the $^{16}\text{O} + ^{16}\text{O}$ scattering as reported by Maher *et al.*⁶ In diagram (a) of the figure we include the original optical-model fit obtained by these authors; in diagram (b) we show the results obtained by Chatwin *et al.*¹⁵ through introduction of a specific dependence of the model parameters on the orbital angular momentum involved; and in diagram (c) we show that an essentially equivalent reproduction of the experimental data can be achieved without necessitating the introduction of the two additional param-

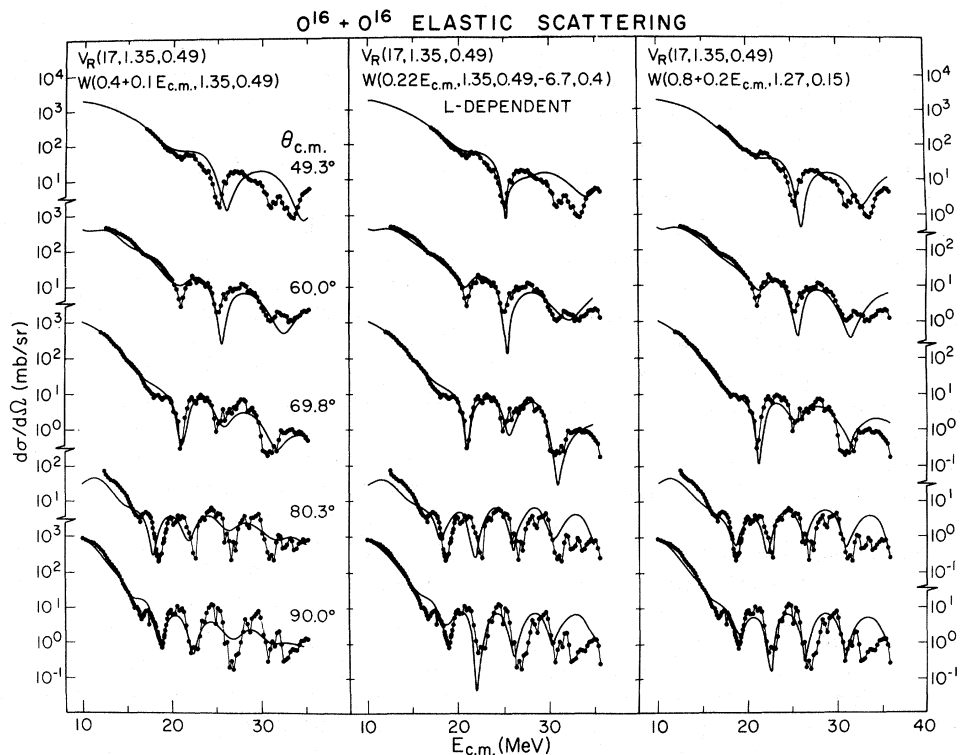


FIG. 3. Optical-model fits to the $^{16}\text{O} + ^{16}\text{O}$ data.

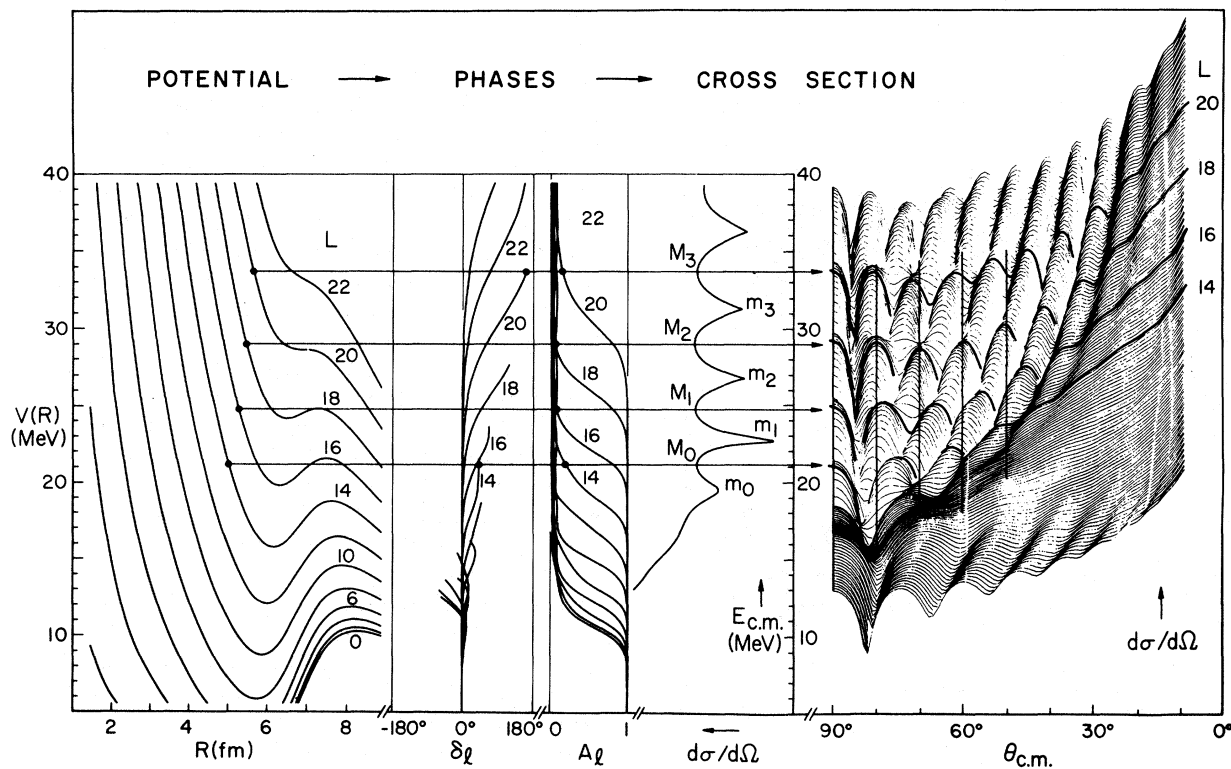


FIG. 4. Optical-model representations of the $^{16}\text{O} + ^{16}\text{O}$ elastic scattering.

eters of the l -dependent model through simple modification of the normal Woods-Saxon parameters describing the absorptive potential. In particular – and it is not physically unreasonable for the double closed ^{16}O nucleus – we have reduced the absorptive diffuseness from 0.49 to 0.15 fm and have further moved the outer edge of the absorptive potential to a smaller radius than that of the real potential. As we shall show below, the essential effects introduced by these two representations – l dependence and reduced imaginary radius – are very closely related. Both favor orbiting and possible resonating of the higher partial waves when compared to the original optical model used by Maher *et al.*

On the basis of such a demonstration we have chosen to focus our attention on the simple Woods-Saxon optical model without any of the modifications which have been suggested by various authors, in an attempt to better understand the detailed nature of this scattering interaction within the simplest possible model framework.

Figure 4 is a schematic representation of the $^{16}\text{O}+^{16}\text{O}$ scattering situation. At the extreme left are shown the real potentials for the different partial waves and for the model parameters appropriate to Fig. 3(c). Unless otherwise specified we shall use this particular model parameter set for all calculations reported herein. Next are

shown the real phase shifts δ_l , and the reflection coefficients A_l , the 90° differential excitation function, and finally an energy-angle map of the calculated elastic scattering corresponding to these same model parameters. In generating this map the model predictions have been reproduced at 0.25-MeV energy intervals.

At low energies, and for corresponding low partial waves, the scattering is characteristic of an absorptive potential in that the corresponding radial wave function is able to penetrate deeply into the nuclear interior and is thus subject to strong absorption. The corresponding phase shifts δ_l are negative. It is worth noting here, and we shall return to it below, that in this energy region just above the Coulomb barrier the smooth cutoff model introduced by McIntyre,³ and which has been applied with considerable success in these energy regions,²⁰ represents a good approximation to the phase shifts which correspond to the complex potential model. With increasing bombarding energy, and hence angular momenta, the internal reflection barrier moves to larger radius where it more strongly affects the radial wave functions and the phase shifts become positive. It should be noted that both the l -dependent potential and that using a reduced imaginary radius and diffuseness enhance this effect. In effect, they increase the absorption of the low angular momentum partial waves while preserving high transparency within the model for those partial waves corresponding to the surface collision.

It should be noted that as each phase shift departs from zero the corresponding reflection coefficient A_l changes quite rapidly from unity to zero. *Each partial wave is thus active over only a relatively restricted range of energy.* This situation is particularly marked in the case of identical particle scattering, since the total absence of the intermediate odd orbital angular momenta implies that at a given energy, at least above some 15 MeV, the scattering is dominated by a single partial wave. This is strikingly evident in the similarity of the calculated angular distribution at the indicated energies to a simple $|P_L(\cos\theta)|^2$ form; this is clearly borne out in the experimental data. In Fig. 4, it is possible to follow the systematic evolution of this behavior. As indicated, the maxima M_0, M_1, M_2 , etc., in the 90° differential cross section at $E_{c.m.} \cong 21, 25, 29$, etc., MeV are attained at the same energy as the $|P_L(\cos\theta)|^2$ angular distribution. As an example, for $L = 18$, $A_{L=18}$ begins to deviate significantly from unity at M_1 and the complete absorption situation for this partial wave is reached at M_2 ; in the interval a deep minimum m_1 at $E_{c.m.} \cong 27$ MeV is generated in the 90° differential cross section

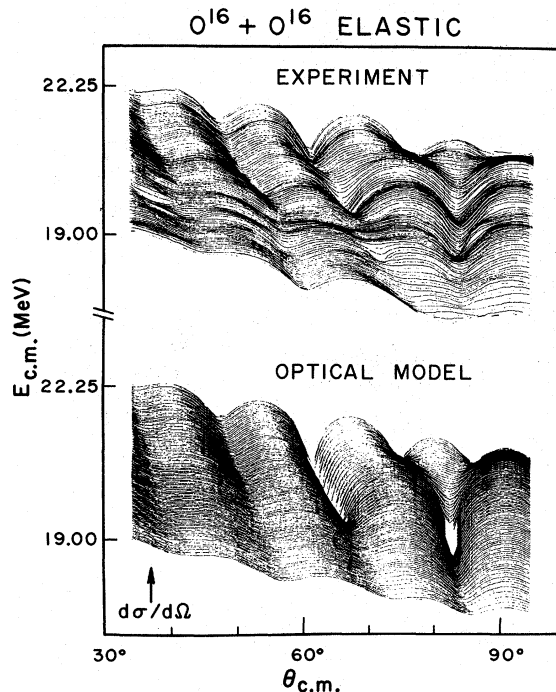


FIG. 5. Optical-model calculations compared with interpolated $^{16}\text{O}+^{16}\text{O}$ data.

when $A_{L=18} \cong 0.5$. A $|P_{L=18}(\cos\theta)|^2$ angular distribution begins to emerge at $E_{c.m.} = 27$ MeV, reaches its clearest definition at $E_{c.m.} = 29$ MeV and disappears to be replaced in turn by the $L = 20$ phenomena.

Inspection of the experimental data on $^{16}\text{O} + ^{16}\text{O}$ in Ref. 6 shows that at the highest energies studied, $E_{c.m.} \cong 40$ MeV, the gross structure in the 90° excitation function was effectively damped out; reference to Fig. 4 shows that such behavior provides strong support for the physical reality of the abnormally shallow real potentials which we have used consistently in our work in this mass region. With a much deeper real well as would be suggested by the discrete ambiguity prescription, for example, the gross structure would be predicted to persist to much higher energies than is observed.

Surface presentations such as that on the right

of Fig. 4 are readily available with even modest computational facilities and, as we have noted above, are of considerable utility in visualizing over-all characteristics of a complex body of data. This is already apparent in Fig. 4 where the vertical heavy lines mark the angles at which the original excitation function data were obtained; from this presentation it is already obvious that at certain energies there is pronounced sensitivity of cross section to small angular changes which readily explain the earlier somewhat puzzling experimental difficulties which were encountered in obtaining consistent experimental data in repeated studies of these regions. The striking transition from Mott scattering to nuclear scattering with increasing energy is also very apparent in this presentation.

In Fig. 5 we illustrate again this utility in con-

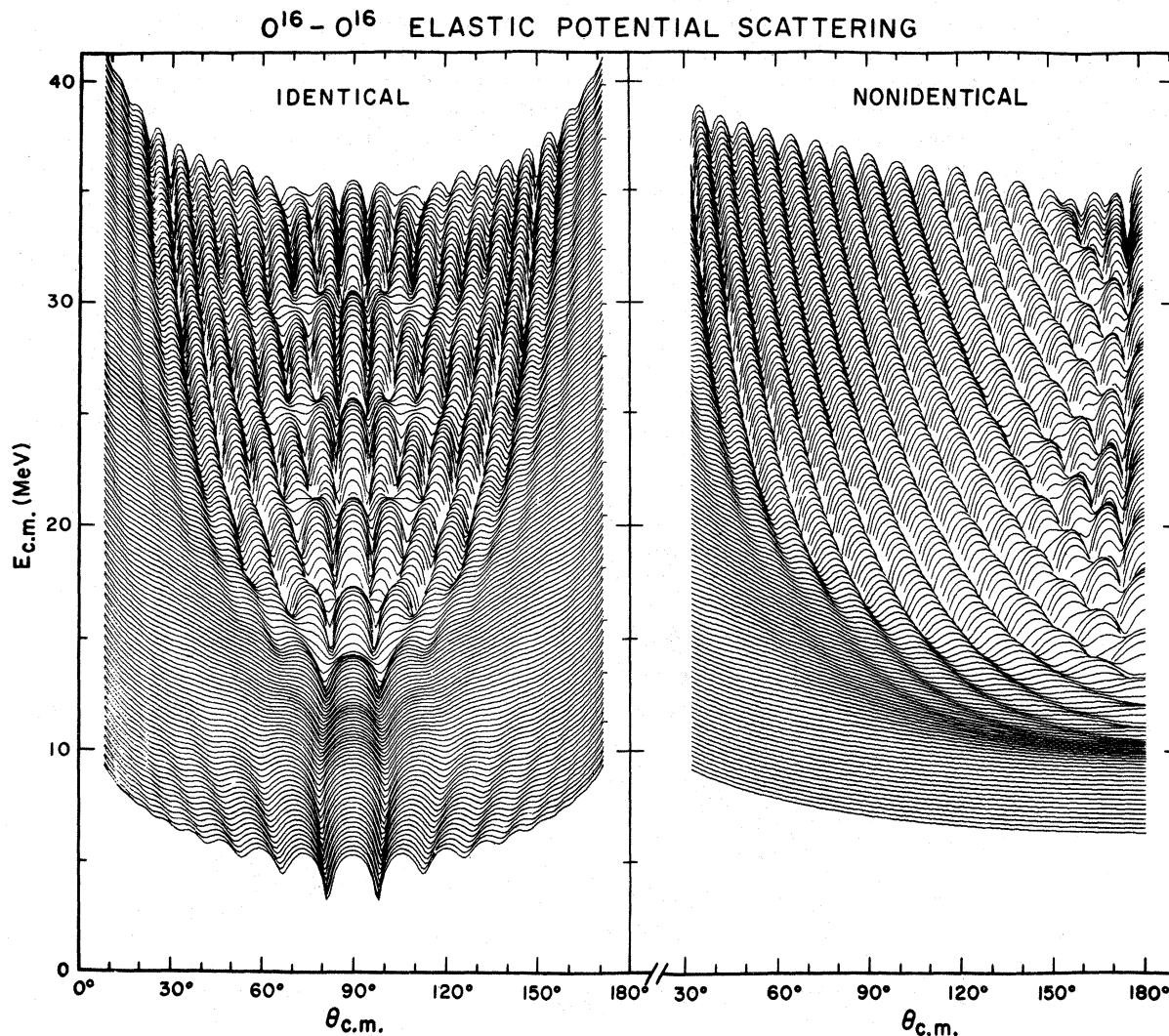


FIG. 6. Optical-model calculations with and without symmetrization.

fronting the model calculations with detailed experimental data measured at narrow energy intervals in the range $19 \leq E_{c.m.} \leq 22.25$ MeV. The gradual evolution of the additional maximum, characteristic of higher P_L^2 , is well reproduced.

Going from an identical to a nonidentical system the predicted energy-angle surface looks, at first sight, completely different as shown in Fig. 6. Here are shown two sets of optical-model predictions for $^{16}\text{O}-^{16}\text{O}$ scattering, where in one case the symmetry due to the scattering of identical particles has been ignored. As we have noted, however, the excitation function for $\theta_{c.m.} = 90^\circ$ has precisely the same shape in both cases. Identical optical-model parameters have been used in both calculations. It is also interesting to note that for nonidentical particles the structure of the excitation functions for $\theta_{c.m.} \sim 180^\circ$ is very similar to the structure at $\theta_{c.m.} \sim 90^\circ$ in the case of identical particles. In the former, however, the number of expected maxima is doubled because not only even but also odd partial waves contribute to the scattering. We have initially focused attention on the identical particle systems for several reasons: The interesting structure at $\theta_{c.m.} \sim 90^\circ$ can be studied where the cross section is large. Only even partial waves contribute to the scattering so that the influence of a single partial wave can be more readily isolated and investigated over a wide energy interval. Compound elastic contributions at $\theta_{c.m.} = 90^\circ$ are also expected to be relatively small compared to the possible contributions at 180° and

finally contributions from exchange processes are possible in these cases only in second order. This follows obviously because to obtain an exit channel identical to the entrance one, an even number of exchange processes must be involved.

On such an energy-angle map the region of sensitivity to surface interaction may be readily recognized; for energies in the region of the Coulomb barrier the region of sensitivity occurs at large angles and moves systematically to very small angles as the bombarding energy is increased. We hope to be able in the future to make use of this systematic probing, with varying energy, in order to permit a systematic extraction of the energy and l dependence of the optical-model parameters.

The region of strong oscillation in the energy-angle map reflects situations where there is strong nuclear interaction and a deep interpenetration of the colliding nuclei.

While the differential cross-section map, as shown in Fig. 6 is largely conditioned by potential scattering surface mechanisms, it can be significantly altered by the presence of resonant or direct elastic amplitudes.²⁰ Figure 7 shows a particularly striking example where inclusion of the elastic neutron transfer amplitude is reflected in a dramatic change in the large angle cross section, even at low energies. The predictions shown in this figure have been obtained from calculations based on the LCNO model for simultaneous elastic scattering and transfer proposed by von Oertzen²¹; they have been confirmed by detailed measure-

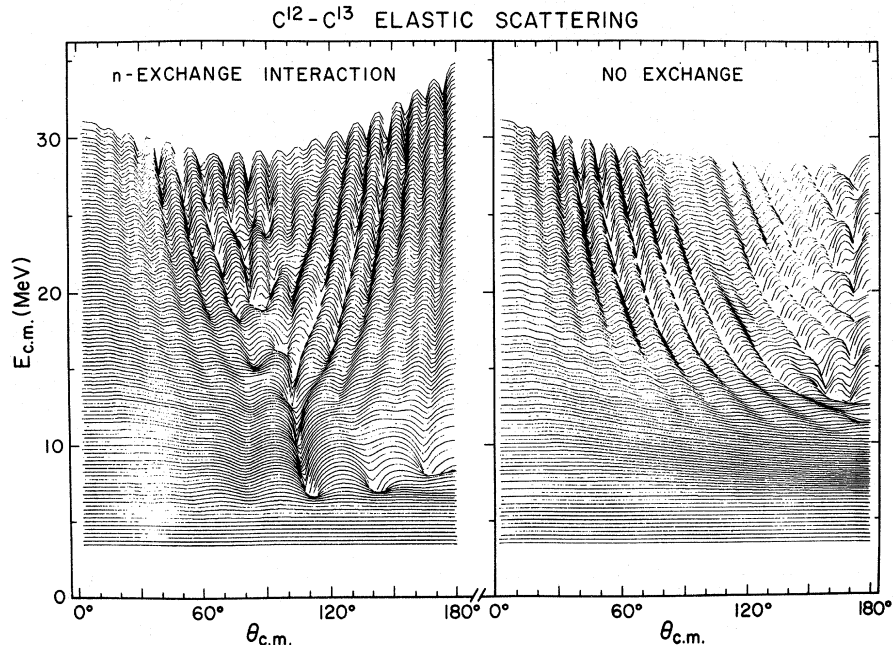


FIG. 7. Model prediction for the $^{12}\text{C}-^{13}\text{C}$ interaction. Plots show $\sigma/\sigma_{\text{ruth}}$ on a logarithmic scale.

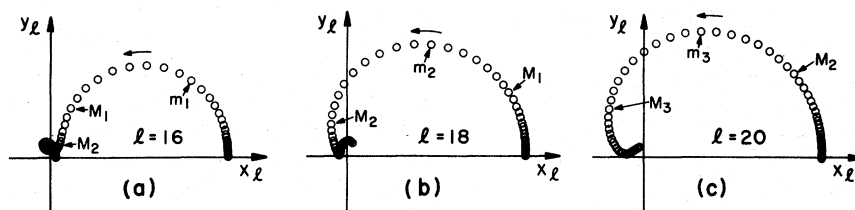
ments on the $^{12}\text{C}-^{13}\text{C}$ system by Chua *et al.*²² in this laboratory. This is a particularly simple situation; in more complex systems, as for example in the case of $^{16}\text{O}-^{12}\text{C}$ scattering, several different phenomena can operate simultaneously to affect the large-angle cross sections. These include both compound elastic contributions and the coupling between elastic scattering and inelastic collective excitations. A further possibility, which has not previously been considered explicitly and

to which we shall return in a subsequent paper,²³ arises from the fact that even and odd partial waves populate even and odd parity states in the compound nuclei involved. This can have a significant impact on the scattering because of the higher characteristic level density for the positive than for the negative-parity states in this region and the fact that correspondingly the even partial waves are more strongly absorbed than are the odd ones. Such a phenomenon can generate an

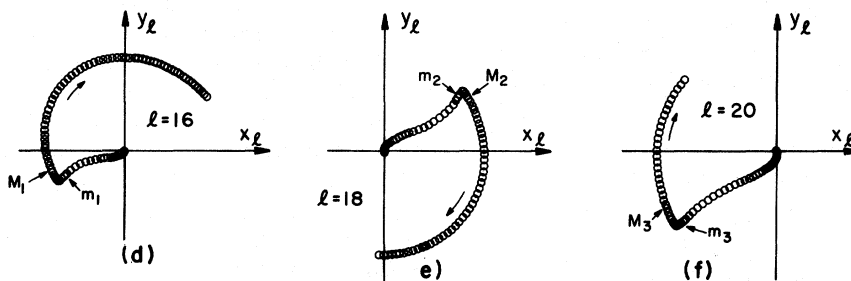
$$\sigma_{el}/\sigma_{Ruth} = \left| i \exp(-i\eta \ln \sin^2 \frac{\theta}{2}) + \frac{\sin^2 \theta/2}{\eta} \sum_{\ell} (2\ell+1) e^{2i(\sigma_{\ell}-\sigma_0)} (1-A_{\ell} e^{2i\delta_{\ell}}) P_{\ell}(\cos \theta) \right|^2$$

$\theta = 90^\circ$

$$X_{\ell}(E) + i Y_{\ell}(E) = A_{\ell} e^{2i\delta_{\ell}}$$



$$X_{\ell}(E) + i Y_{\ell}(E) = \frac{1}{2\eta} (2\ell+1) e^{2i(\sigma_{\ell}-\sigma_0)} (1-A_{\ell} e^{2i\delta_{\ell}}) P_{\ell}(0)$$



$$X_T(E) + i Y_T(E) = i \exp(-i\eta \ln 2) + \frac{1}{2\eta} \sum_{\ell} (2\ell+1) e^{2i(\sigma_{\ell}-\sigma_0)} (1-A_{\ell} e^{2i\delta_{\ell}}) P_{\ell}(0)$$

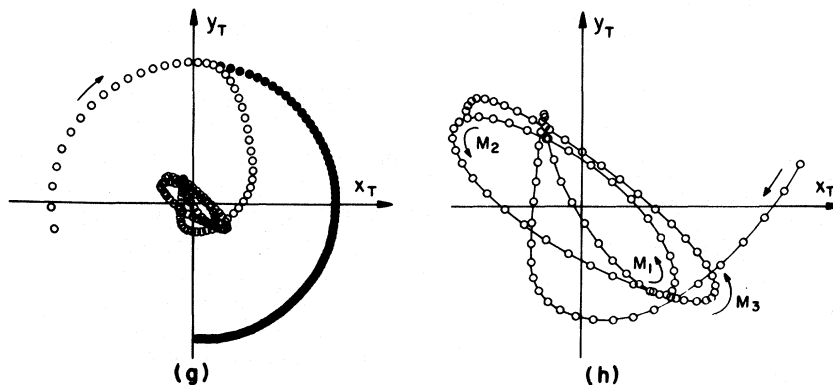


Fig. 8. (a)-(h) Vector diagrams for identical particle elastic scattering.

even-odd effect similar to that observed in the elastic transfer situation and can again give rise to an increase in large-angle cross sections in the scattering.

IV. PHASE-SHIFT BEHAVIOR

Returning to the identical particle case, it is possible to obtain a fuller understanding of the behavior of individual partial waves in the scattering through construction of the familiar Argand diagrams shown in Fig. 8. Here the behavior of the $L = 16, 18,$ and 20 partial waves, as shown in Fig. 4, is examined in detail. In diagrams (a), (b), and (c) the function $A_l e^{2i\delta_l}$ is displayed, whereas in diagrams (d), (e), and (f) the function $1 - A_l e^{2i\delta_l}$ is displayed through simple translation of the origins to $X_l = 1$ and $Y_l = 0$. These latter three partial wave amplitude plots display very similar features.

At the energy where a given partial wave begins to contribute significantly to the cross section a fast rise in the partial amplitude and almost no change in phase is observed. With increasing energy a region occurs wherein the partial amplitude is stationary because the Coulomb and nuclear phase shifts move in opposite directions.

To illustrate how the 90° excitation function is generated in the energy interval $20 \leq E_{c.m.} \leq 34$ MeV we consider the $L = 20$ partial wave. This first deviates from zero at $E_{c.m.} \cong 20$ MeV where all the lower L amplitudes are essentially vectors of constant length moving with the Coulomb phase;

these amplitudes add coherently with the first term of unit length to form a smoothly varying background (Coulomb phase shifts vary smoothly with energy). The magnitude of the $L = 20$ partial wave increases rapidly with energy interfering destructively with the background. After the minimum m_3 is reached the $L = 20$ amplitude remains essentially constant, but the background phase varies so that the cross section again increases.

The last two diagrams [Figs. 8(g) and 8(h)] display the total scattering amplitude. At low energies the Coulomb term dominates. However, at higher energies the interference of different partial waves reduces the cross section. The origin of the oscillations in the 90° differential cross section are particularly evident in Fig. 8(h), which is an enlargement of the central region of Fig. 8(g).

For a better understanding of the mechanism generating the shape displayed by the Argand diagrams (a), (b), and (c) of Fig. 8 we have systematically decreased the magnitude of the imaginary part of the complex potential in order to magnify the shape effects caused by the real potential. The results obtained for the $l = 18$ partial wave are given in Fig. 9: $c = 1$ represents the starting situation of Fig. 8(b); for $c = 0$ the absorptive imaginary part has been completely eliminated; as expected the real phase moves, as a function of the energy, along the unitary radius. It is interesting to note that for $c = 0$ an almost perfect resonancelike behavior is observed, with a slow change of the phase at the extreme energies and a much more rapid change in the region of $\delta = 90^\circ$. This energy corresponds to the minima m_2 of Fig. 4, where the $l = 18$ partial wave is affected by a rapid change in the shape of the corresponding potential barrier. The effect of the increasing imaginary potential in masking this classic resonance behavior is obvious in Fig. 8.

It is convenient to parametrize such resonances in terms of a modified Breit-Wigner amplitude; the modification involves the addition of a background term, giving for the complete amplitude

$$S(E) = \left(\frac{a+ib}{E-E_0+i\Gamma_T} + u+iv \right) A(E). \quad (1)$$

It must be noted that in contrast to the usual situations wherein Breit-Wigner formalism is used, here the background changes rapidly over the energy width of the resonance. We have chosen to account for this background variation by introducing the smooth cutoff function:

$$A(E) = \left[1 + \exp\left(\frac{E-\bar{E}_0}{\Delta\bar{E}_0}\right) \right]^{-1}. \quad (2)$$

We have introduced the complex term $u+iv$ in Eq.

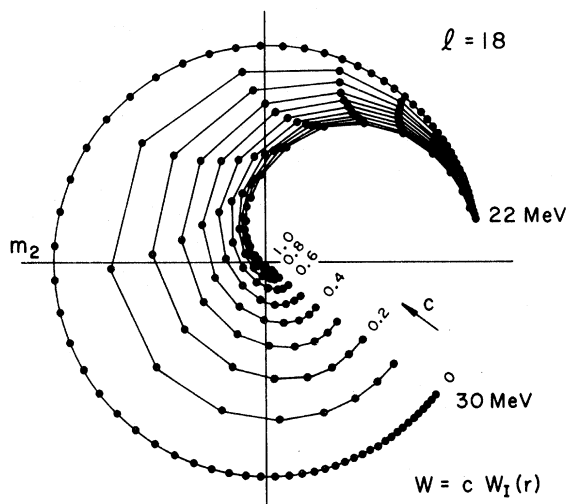


FIG. 9. Argand diagram displaying the energy dependence of the scattering function for $l = 18$ for an imaginary potential of variable magnitude.

(1) to account for the residue of the resonance and to preserve a reasonable asymptotic behavior for the resonant tails at large energy separation from the resonant peak.

Such a parametrization leads to difficulties in describing the low-energy tails of the resonance. The presence of both Coulomb and centrifugal barriers preclude any sensitivity to the resonance at low bombarding energies, and in consequence the resonance prescription fails to reproduce accurately the asymptotic part of the phase shift on which the scattering problems depend sensitively.

In order to avoid this problem we have examined a further parametrization very reminiscent of that used by McIntyre and his collaborators³ which assumes a scattering amplitude of the following form:

$$S(E) = A(E)\exp[\delta(E)], \quad (3)$$

where $A(E)$ is as specified above and

$$\delta(E) = \delta_0 \left[1 + \exp\left(\frac{E' - E}{\Delta E'}\right) \right]^{-1}. \quad (4)$$

$\delta(E)$ is introduced to reproduce the energy behavior of the real nuclear phase shifts. In Fig. 10 we compare, for the $l=18$ partial waves, the scattering amplitudes obtained with the optical-model parametrization with the modified Breit-Wigner parametrization and with this last smooth cutoff

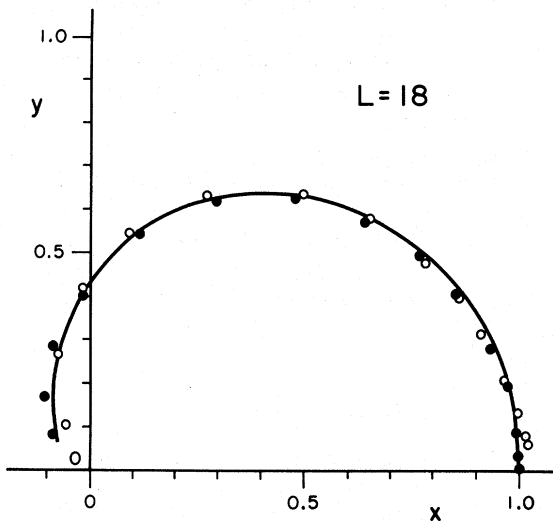


FIG. 10. Argand diagram of energy dependence of the $L=18$ partial wave. The solid line is the optical-model prediction using the parameter set of Fig. 3(c). Open circles are due to the Breit-Wigner resonance fit [$\Gamma_{i,f} = (a^2 + b^2)^{1/2} = 3.63$, $E_0 = 25.76$, $\Gamma_T = 3.66$, $u = 0.67$, $v = -0.117$, $\bar{E}_0 = 23.90$, $\Delta\bar{E}_0 = 2.52$]. Full dots were obtained through the smooth cutoff parametrization ($\bar{E}_0 = 26.2$, $\Delta\bar{E}_0 = 0.94$, $\delta_0 = 3.62$, $E' = 26.8$, $\Delta E' = 1.7$).

parametrization. As is obvious from the figure, the three parametrizations give almost identical results.

The Breit-Wigner parametrization, however, permits the extraction of both a total and a partial width for the resonance phenomena. The lifetime associated with the total width $\Gamma_T = 3.66$ MeV, thus extracted, is 4.6×10^{-22} sec – a time characteristic of a direct process. The $l=18$ resonance is predicted to fall at 25.8 MeV. This falls just above the $l=18$ potential barrier as expected from earlier more general arguments.

Figure 11 shows the wave function for $L=18$ as function of distance and energy in the $^{16}\text{O} + ^{16}\text{O}$ scattering interaction as calculated on an optical-model basis. The increase of the radial wave function just above the barrier indicates the resonance phenomena which we discuss herein. This is the most critical region of the heavy-ion interaction, and as evident here it is dominated by a surface mechanism where the collision time is relatively long and possible orbiting can occur. It should be noted that this orbiting condition has much in common with a metastable quasimolecular state; a transition from the orbiting condition to a more strongly bound quasimolecular state, as is implied in a number of the mechanisms which have been suggested to explain the intermediate structure in the scattering data,²⁴ is thus a natural one.

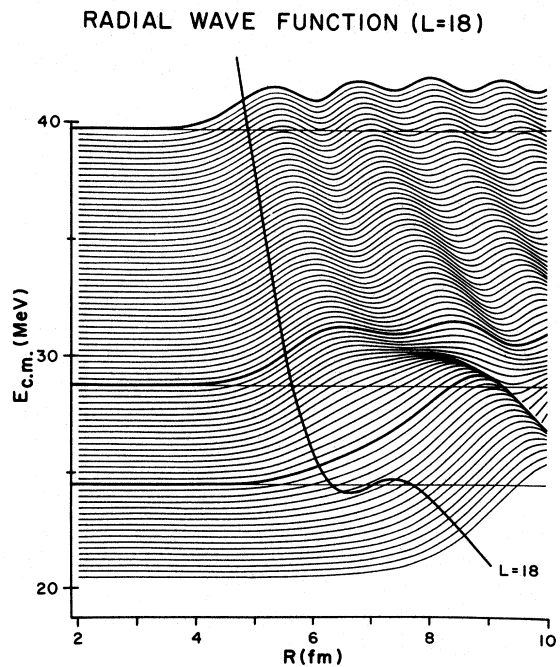


FIG. 11. Radial wave function ($L=18$). The dark solid line represents the real potential for $L=18$.

An extension of this approach follows in analogy with the familiar DWBA calculations where overlapping of wave functions of different reaction channels is invoked. It is clear that a large amplitude for one single partial wave at energies just above the attractive part of the potential will favor situations with flux going to surface phenomena such as inelastic scattering or transfer reactions (good overlap between wave functions). Equivalently, elastic scattering receives strong contributions from the surface effects if the matching conditions of energy and angular momentum are favorable.^{25, 26}

It follows from all of this that within the framework of an optical model it is possible to identify specific energy and angular behavior of the elastic channels with particular partial waves. However, the classical resonance behavior is masked by the absorption present.

V. POSSIBLE VARIABLE MOMENT OF INERTIA OF THE INTERACTING SYSTEM

Granting that the optical model can be shown to provide a convenient and reasonably successful parametrization of the heavy-ion scattering interaction, its physical justification is still not firmly established. One of the serious omissions from typical optical-model considerations, for example, is that of nuclear superfluidity to the extent that the nuclear matter involved can be in a superfluid state when two heavy ions overlap significantly during their interaction. Their total moment of inertia may depart markedly from a simple two-sphere approximation if the central volume of the system can be uncoupled, through superfluidity, from over-all rotation of the complete system. In such a picture a variable moment of inertia would be required in the interaction Hamiltonian and the effective centrifugal barriers would be correspondingly altered for different partial waves.

The $^{16}\text{O} + ^{16}\text{O}$ scattering situation is an attractive one for searching for possible occurrence of such superfluidity effects. The scattering is only weakly absorptive for large l values – after admitting significant interpenetration of the scattering ions. As we have shown, single partial waves are dominant in given energy regions in the scattering and in consequence the energy dependence of the differential cross section is expected to be extremely sensitive to the characteristics of the centrifugal barriers involved and, in consequence, to any superfluidity effects which might result in the modification of these barriers.

In order to examine this phenomenon we have used an energy-dependent parametrization of the McIntyre type, as discussed above, to predict the L

$= 14, 16, 18, 20,$ and 22 nuclear phase shifts for the $^{16}\text{O} + ^{16}\text{O}$ problem. The behavior of the remaining l values in the range from 0 to 30 were taken from simple optical-model calculations. With this complete set of predicted phase shifts a least-squares fit was performed to the $^{16}\text{O} - ^{16}\text{O}$ scattering data; the results are displayed in Fig. 12(a). It is very important to note that, in contrast to a standard optical-model calculation, here the energy value, where the different partial waves begin to deviate from $A_l = 1$, $\delta_l = 0$, is not uniquely fixed by the centrifugal energy term $l(l+1)\hbar^2/2mR^2$. These energies, in the present approach, can be varied freely during the least-squares-fitting procedure so that the phase-shift behavior can be extracted directly from the experimental observations. In Fig. 12(b) we have displayed the results of this examination; the phase-shift behavior given by a standard optical-model calculation is compared with that obtained through the direct

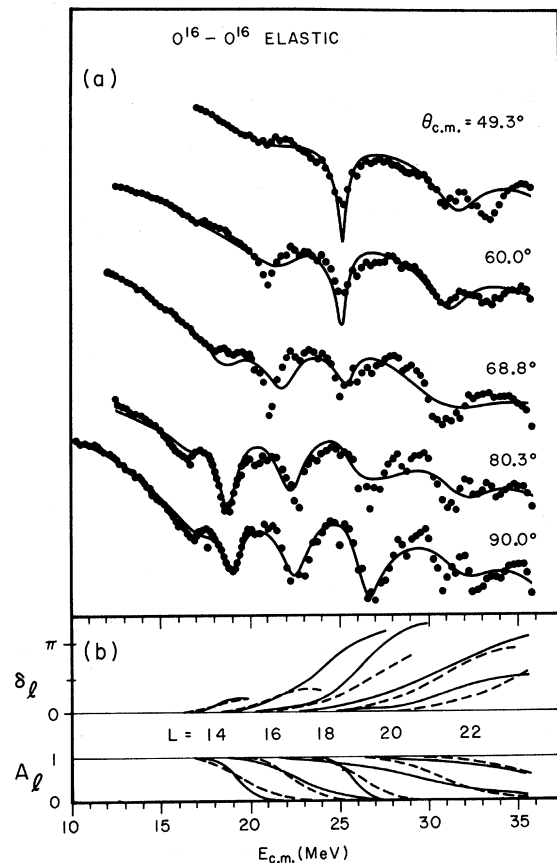


FIG. 12. Direct extraction of the nuclear phase shift from the $^{16}\text{O} - ^{16}\text{O}$ data: (a) Least-squares fit results using a smooth cutoff parametrization. (b) The solid lines are the nuclear phases extracted from the optical-model calculation. The dashed lines are the results of the smooth cutoff parametrization.

parametrization which we have just described. No systematic difference between the two parametrizations appears despite the additional degrees of freedom given in the direct parametrization.

While this provides further support for the utility of the optical-model approach in the description of these heavy-ion scattering interactions, it provides no evidence for any variable-moment-of-inertia effects. It should be emphasized, however, that the fact that the moment of inertia does not appear to vary in the ^{16}O - ^{16}O case, which we have examined here, certainly does not preclude the appearance of such effects in moving to heavier nuclear systems. The search for such effects will be of particular interest when these heavier systems become experimentally accessible to precision scattering studies.

VI. DEPENDENCE OF THE IMAGINARY POTENTIAL ON ANGULAR MOMENTUM, ENERGY, AND MASS SYSTEM

As has been discussed previously, the real part of the complex potential, and especially its exterior part, can be extracted with good precision

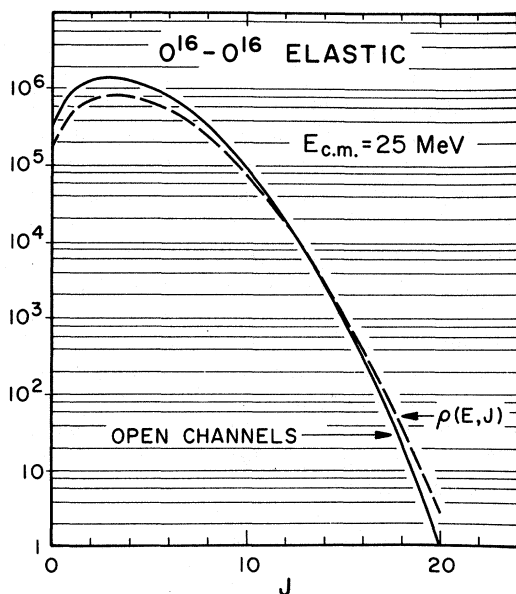


FIG. 13. The level density $\rho(E, J)$ is calculated using the formula of Ref. 31 where the parameters are taken to be $\alpha = 0.125$ and the moment of inertia has the value of a rigid sphere of radius $R = 1.2A^{1/3}$ fm. The number of open channels is calculated using a zero-to-unity step function for the barrier penetrability as calculated in a pure Coulomb scattering situation for a Fermi radius of $R = 1.5A^{1/3}$. The level density in the residual nucleus is calculated as given above.

from the experimental data; no real necessity for an l or E dependence seems to be required. For the imaginary part, however, an energy as well as an l dependence seems to be necessary to reproduce the experimental observations. If we consider, for example, the results displayed in Fig. 1, it appears that the magnitude of the scattering cross section reflects from case to case a rather different strength for the absorption of the ingoing flux. In the ^{18}O - ^{18}O scattering especially, the cross section appears to be very much damped by a strong absorption. In order to provide the optical model with a predictive power for the analysis of new systems, it is important to understand how the ingoing flux is absorbed and how it is distributed among all the outgoing channels. A detailed analysis of this problem will be given in a subsequent paper²³ and we shall concentrate here on a brief summary. Heavy-ion reactions are generally dominated by energy and angular momentum conservation and barrier penetration effects. On a time scale, as is well known, the processes can be separated into direct and compound reactions. Direct processes imply a surface absorption, compound processes imply a volume absorption, and thus, the imaginary potential should consist of these two terms. The former represents the flux going to transfer reactions, inelastic collective excitations, and break-up reactions; the strength depends primarily on the structure of the colliding nuclei (separation energy of the last nucleons, deformation, etc.) and is expected to increase strongly at energies above the Coulomb barrier. The ideal solution would be to include the direct channels explicitly in a coupled-channel calculation,²⁷ but this is practically impossible especially when searching for optical-model parameters. No strong l dependence is usually expected for this part of the potential although in special cases the selection rules of the direct processes may cause even-odd effects as mentioned earlier.

The situation is very much different in the case of the compound reactions which of course are dominated by the structure of the compound nucleus. Because of the reaction Q value and the very large rapidly varying amount of angular momentum introduced by heavy projectiles in the nuclear interaction, the number of open channels and the availability of compound states can change drastically from mass system to mass system, or as a function of the angular momentum and of the bombarding energy involved. As an example, Fig. 13 illustrates the number of open channels and the number of levels per MeV in the compound nucleus, as functions of the angular momentum involved, for a selected case (the ^{16}O - ^{16}O interaction) at a

fixed bombarding energy. Chatwin *et al.*¹⁵ introduced into the heavy-ion scattering problem an l -dependent imaginary potential of the form

$$W = W_0 \{1 + \exp[(l - l_c)/\Delta l]\}^{-1}, \quad (5)$$

where l_c and Δl are, for a given energy interval, constants estimated on the basis of the number of open channels. However, both the number of open channels and the level density in the compound nucleus are expected to be dominant factors. Formation and decay of the compound nucleus are not independent and a rather complicated dependence

of W on these quantities might be expected. The advantage of this extended approach, if such a dependence can be found, lies in the fact that the level density and number of open channels can be predicted rather easily for different systems and only few parameters are involved (e.g., the moment of inertia θ and the nuclear temperature parameter a which can be extracted from other experimental data²⁸).

In an attempt to find a general dependence of W on energy, angular momentum, and mass system, we have first assumed that only the formation of the compound nucleus is determinant and that all levels in the compound nucleus have equal probability of being populated:

$$W = C\rho(E, l)V_{\text{real}}(r) + W_{\text{surf}}. \quad (6)$$

The radial dependence of the compound-reaction part of the absorption is chosen to be identical to the Woods-Saxon form of the real potential; $\rho(E, l)$ is the level density in the compound nucleus and C is a constant adjusted to the experimental data.

The surface absorption, W_{surf} , describing the direct processes was chosen to have a quadratically increasing energy dependence (starting at the height of the Coulomb barrier) and a radial dependence given by the derivative of a Woods-Saxon form factor.

The results of the calculations as applied to the ^{16}O - ^{16}O scattering are shown in Fig. 14. The fit is particularly good at the small scattering angles, where the standard optical model usually fails.

Not fully satisfactory is the fit at large angles and at low energy which probably reflects a too drastic l dependence of the model as it now stands. This last observation has been confirmed by calculations applied to similar mass systems.

An analogous approach has been proposed recently by Greiner *et al.*²⁹ and by Low and Tamura.³⁰ The general trend of these modifications to be applied to the standard optical model appears promising although a better derivation of the functional dependence of W on the average nuclear parameters is badly needed.

VII. CONCLUSIONS

We have presented herein a detailed study of available heavy-ion excitation function and angular-distribution data within an optical-model framework in an attempt both to arrive at reasonable optical-model parameters and to understand the origin of the gross structure observed in the excitation function data. The existence of orbiting resonances has been demonstrated for the ^{16}O - ^{16}O scattering.

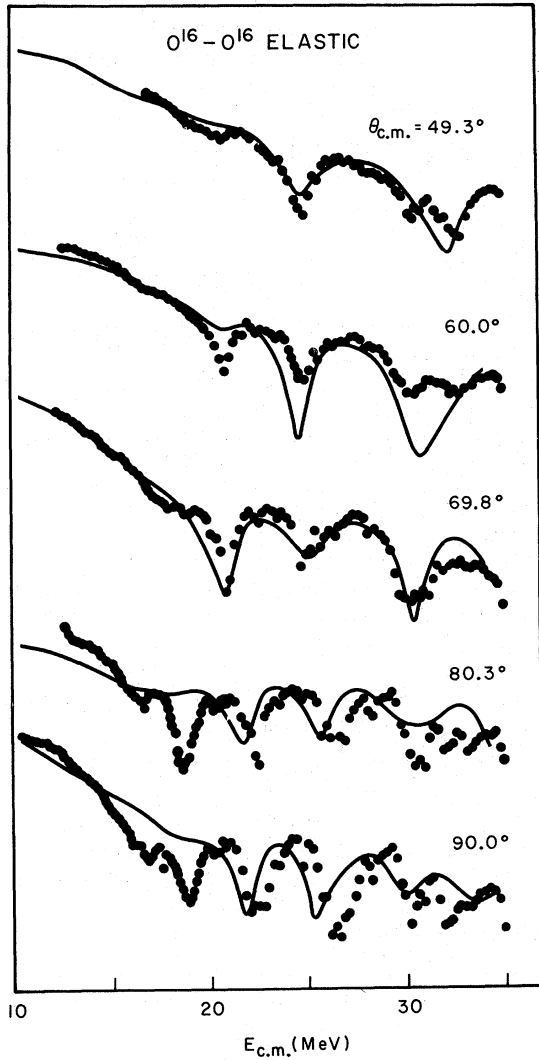


FIG. 14. Optical-model fit obtained with an imaginary potential strength proportional to the level density in the compound nucleus. ($C=0.01$.) The real potential parameters are: $V=17$ MeV, $r_0=1.35$, $a=0.49$. The parameters of the surface absorption are: $W=-0.2+0.002E_{\text{c.m.}}^2$, $r_0=1.35$, $a=0.6$.

Possible consequences of these interesting phenomena, which can serve as doorway states for the population of quasimolecular type of configurations and direct processes, have been indicated. The low absorption of the grazing partial waves has been understood as a reflection of the particularly low density of states in the corresponding compound nucleus.

Need for modification of the optical model has been indicated. No evidence of a variable moment of inertia has been found in the ^{16}O - ^{16}O system. A preliminary study involving the derivation of the dependence of the imaginary optical potential on the average properties of the nuclei involved has been reported.

We conclude that the potential scattering aspects of the elastic interaction are now reasonably well

understood at least in the nuclear mass region which has thus far been accessible to study. The situation concerning the more complex phenomena involved in the elastic interaction, e.g., coupling, double resonances, elastic transfer, etc., remains much more open; in subsequent papers we shall discuss these in turn.

ACKNOWLEDGMENTS

The authors wish to acknowledge many stimulating discussions with R. Stokstad, G. H. Rawitscher, and R. Ascutto. We are much indebted to M. W. Sachs for providing us with excellent computational facilities. Mrs. Hana Novak has been most helpful in preparing the illustrations used herein.

*Work supported under U. S. Atomic Energy Commission Contract No. AT(11-1)3074.

†Present address: Gesellschaft für Schwerionenforschung mbH, 6100 Darmstadt 1, West Germany.

¹K. W. Ford and J. A. Wheeler, *Ann. Phys. (N.Y.)* **1**, 259 (1959).

²D. Robson, Argonne National Laboratory Report No. ANL-7837, 1971 (unpublished).

³J. A. McIntyre, K. H. Wang, and L. C. Becker, *Phys. Rev.* **117**, 1337 (1960).

⁴D. A. Bromley, in *Nuclear Structure and Nuclear Reactions, Proceedings of the International School of Physics "Enrico Fermi," Course XL*, edited by M. Jean and R. A. Ricci (Academic, New York, 1969), p. 242.

⁵A. Gobbi, in *Proceedings of the Symposium on Heavy Ion Scattering*, Argonne National Laboratory Report No. ANL-7837, 1971 (unpublished).

⁶J. V. Maher, M. W. Sachs, R. H. Siemssen, A. Weidinger, and D. A. Bromley, *Phys. Rev.* **188**, 1665 (1969); J. V. Maher, Doctoral Dissertation, Yale University, 1969 (unpublished).

⁷D. A. Bromley, J. A. Kuehner, and E. Almqvist, *Phys. Rev.* **123**, 878 (1961).

⁸R. W. Shaw, R. Vandenbosch, and M. K. Mehta, *Phys. Rev. Letters* **25**, 457 (1970).

⁹R. H. Siemssen, H. T. Fortune, R. Malmin, A. Richter, J. W. Tippie, and P. P. Singh, *Phys. Rev. Letters* **25**, 536 (1970).

¹⁰L. A. Jacobson, *Phys. Rev.* **188**, 1509 (1969).

¹¹W. Reilly, R. Wieland, A. Gobbi, M. W. Sachs, and D. A. Bromley, in *Proceedings of the International Conference on Nuclear Reactions Induced by Heavy Ions, Heidelberg, 1969*, edited by R. Bock and W. R. Hering (North-Holland, Amsterdam, 1970), p. 93.

¹²W. Reilly, R. Wieland, A. Gobbi, M. W. Sachs, J. V. Maher, D. Mingay, R. H. Siemssen, and D. A. Bromley, in *Proceedings of the International Conference on Nuclear Reactions Induced by Heavy Ions, Heidelberg, 1969* (Ref. 11), p. 95.

¹³G. C. Morrison, H. T. Fortune, and R. H. Siemssen, in *Proceedings of the International Conference on Nuclear Reactions Induced by Heavy Ions, Heidelberg, 1969* (Ref. 11), p. 72.

¹⁴W. Scheid, R. Ligensa, and W. Greiner, *Phys. Rev. Letters* **21**, 1479 (1968).

¹⁵R. A. Chatwin, J. S. Eck, D. Robson, and A. Richter, *Phys. Rev. C* **1**, 795 (1970).

¹⁶L. Rickertsen, B. Block, J. W. Clark, and F. B. Malik, *Phys. Rev. Letters* **22**, 951 (1969).

¹⁷J. S. Blair, in *Proceedings of the International Conference on Nuclear Reactions Induced by Heavy Ions, Heidelberg, 1969* (Ref. 11) p. 1.

¹⁸K. W. McVoy, *Phys. Rev. C* **3**, 1104 (1971).

¹⁹W. E. Frahn, *Phys. Rev. Letters* **26**, 568 (1971).

²⁰A. Gobbi, U. Matter, J. L. Perrenoud, and P. Marmier, *Nucl. Phys.* **A112**, 537 (1968).

²¹W. von Oertzen, *Nucl. Phys.* **A148**, 529 (1970).

²²L. Chua, R. Stokstad, A. Gobbi, P. Parker, M. Sachs, D. Shapira, R. Wieland, and D. A. Bromley, *Bull. Am. Phys. Soc.* **17**, 529 (1972).

²³A. Gobbi *et al.*, to be published.

²⁴W. Greiner and W. Scheid, *J. Phys. (Paris) Suppl.* **32**, Fasc. 11-12, C.G.-91 (1971).

²⁵P. H. Barker, A. Huber, H. Knoth, U. Matter, A. Gobbi, and P. Marmier, *Nucl. Phys.* **A155**, 401 (1970).

²⁶P. J. A. Buttle and L. J. B. Goldfarb, in *Proceedings of the International Conference on Nuclear Reactions Induced by Heavy Ions, Heidelberg, 1969* (Ref. 11), p. 197.

²⁷R. J. Ascutto and N. K. Glendenning, *Phys. Rev.* **181**, 1396 (1969).

²⁸T. D. Thomas, *Ann. Rev. Nucl. Sci.* **18**, 343 (1968).

²⁹H.-J. Fink, W. Scheid, and W. Greiner, *Nucl. Phys.* **A188**, 259 (1972).

³⁰K. S. Low and T. Tamura, *Phys. Letters* **40B**, 32 (1972).

³¹D. W. Lang, *Nucl. Phys.* **42**, 353 (1963).